Biomaterials 69 (2015) 174–183

Contents lists available at ScienceDirect

Biomaterials

journal homepage: www.elsevier.com/locate/biomaterials

Geometric guidance of integrin mediated traction stress during stem cell differentiation

Junmin Lee [a, b], Amr A. Abdeen [a, b], Xin Tang [b, c], Taher A. Saif [b, c], Kristopher A. Kilian [a, b, *]

[a] Department of Materials Science and Engineering, University of Illinois at Urbana-Champaign, IL 61801, USA
[b] Micro and Nanotechnology Laboratory, University of Illinois at Urbana-Champaign, IL 61801, USA
[c] Department of Mechanical Science and Engineering, University of Illinois at Urbana–Champaign, Urbana, IL 61801, USA

ARTICLE INFO

Article history:
Received 31 July 2015
Accepted 4 August 2015
Available online 5 August 2015

Keywords:
Mesenchymal stem cells
Differentiation
Microenvironment
Traction stress
Integrin

ABSTRACT

Cells sense and transduce the chemical and mechanical properties of their microenvironment through cell surface integrin receptors. Traction stress exerted by cells on the extracellular matrix mediates focal adhesion stabilization and regulation of the cytoskeleton for directing biological activity. Understanding how stem cells integrate biomaterials properties through focal adhesions during differentiation is important for the design of soft materials for regenerative medicine. In this paper we use micropatterned hydrogels containing fluorescent beads to explore force transmission through integrins from single mesenchymal stem cells (MSCs) during differentiation. When cultured on polyacrylamide gels, MSCs will express markers associated with osteogenesis and myogenesis in a stiffness dependent manner. The shape of single cells and the composition of tethered matrix protein both influence the magnitude of traction stress applied and the resultant differentiation outcome. We show how geometry guides the spatial positioning of focal adhesions to maximize interaction with the matrix, and uncover a relationship between αvβ3, α5β1 and mechanochemical regulation of osteogenesis.

1. Introduction

Stem cells in their niche are in contact with the extracellular matrix (ECM) which provides multiple structural and biochemical cues to direct their behavior [1–8]. Cells adhere to the ECM through several different cell surface receptors including integrins which are involved in mechanosensing and bi-directional transmission of mechanical force [9]. This interaction allows cells to sense and respond to their microenvironment via contractile forces and to adaptively remodel tissues with dynamic mechanical forces, guiding broad aspects of their functions such as cell migration, growth, differentiation, and survival [10–15]. For this reason, the careful design of the cellular recognition interface on deformable biomaterials is a critical aspect for the regulation of distinct stem cell functions.

Mesenchymal stem cells (MSCs) are multipotent cells which have the ability to differentiate into several cell types including chondrocytes, adipocytes, myoblasts and osteoblasts in vitro, and this process is regulated by biophysical and biochemical dynamics of signal-activated gene regulation [16–25]. Controlling the microenvironment properties such as matrix elasticity [17,26,27], cell and tissue shape [19,28,29], and adhesive proteins [20,30] can regulate lineage specification of MSCs. For example, MSC lineage specification to neurogenesis, myogenesis, or osteogenesis outcomes can be directed by matrix elasticity [17]. Specifically, MSCs cultured on stiff substrates (~34 kPa), which promote cell spreading, are guided to an osteogenesis outcome due to increased contractility of the actomyosin cytoskeleton. Cytoskeletal tension can be modulated not only by matrix elasticity but also by cell shape. For instance, cells cultured in shapes which promote cytoskeletal tension prefer to adopt an osteogenic fate while those in relaxed shapes prefer to undergo adipogenesis [19,31]. In addition, MSC osteogenesis can be tuned on fibronectin coated substrates with variable stiffness (10–40 kPa) by controlling the geometry of single micropatterned cells [29]. Other reports have shown that combining different adhesion ligands (fibronectin, laminin, or collagen) with hydrogels of variable matrix elasticity, influences MSC differentiation between osteogenesis and myogenesis lineages [21].

MSCs interact with extracellular matrix proteins through various integrins including α1-6, αV, α11, αX, β1-4, and β7-8 [10,13]. Combinations of two different chains, integrin α and β subunits, define the surface receptors that recognize ECM proteins such as: fibronectin, vitronectin, collagen, and laminin [32,33]. These integrin

* Corresponding author. Department of Materials Science and Engineering, University of Illinois at Urbana-Champaign, IL 61801, USA.
E-mail address: kakilian@illinois.edu (K.A. Kilian).

http://dx.doi.org/10.1016/j.biomaterials.2015.08.005
0142-9612/

transmembrane receptors act as mechanosensors and mechanotransducers to connect the actin cytoskeleton to the ECM and enable dynamic interactions with the microenvironment through focal adhesions. For example, MSCs primarily bind to fibronectin through the common integrin heterodimers α5β1 or αVβ3 [34]. A previous report showed that α5 integrin expression in MSCs was elevated during osteogenic differentiation while cells expressed higher level of α6 integrin during adipogenic lineage specification at 7 days [10]. The surface geometry and local biochemical microenvironment of biomaterials have been shown to influence focal adhesions, cytoskeletal tension and differentiation in adherent MSCs [19]. However, the relationship between integrin mediated traction stress and MSC differentiation has not been described.

In this paper we show how control of cell shape can be used to study the relationship between focal adhesion, traction stress, and the differentiation of single mesenchymal stem cells. We use immunofluorescence staining to investigate the protein expression of key markers during osteogenesis and myogenesis. Traction stress measurements are employed to assess the force generated by MSCs with different combinations of these cues. We show through immunofluorescence that the expression of early and late osteogenic markers is dependent on the engagement of α5β1 and αVβ3 integrins.

2. Materials and methods

2.1. Materials

All materials were purchased from Sigma unless otherwise noted. Tissue culture plastic ware and glass coverslips (18-mm circular) were purchased from Fisher Scientific. Cell culture media and reagents were purchased from Gibco. Rabbit anti-Runx2 (ab23981) and anti-Osteopontin (ab8448) were purchased from Abcam. Mouse anti-MyoD (MAB3878) Mouse anti-α5β1 (MAB1969) and αVβ3 (MAB1976Z) were purchased from Millipore. Blebbistatin, Y-27632, FR180204 (ERK inhibitor), SP600125 (JNK inhibitor), and SB202190 (p38 inhibitor) were purchased from Calbiochem. Tetramethylrhodamine-conjugated anti-rabbit IgG antibody, Alexa Fluor 647-conjugated anti-mouse IgG antibody, Alexa Fluor 555-conjugated anti-rabbit IgG antibody, Alexa488-phalloidin and 4,6-diamidino-2-phenylindole (DAPI) were purchased from Invitrogen.

2.2. Surface preparation

Polyacrylamide substrates were prepared as previously described [29]. Briefly, 10–40 kPa stiffness gels were made by using mixtures of acrylamide/bis-acrylamide according to the desired stiffness [35]. For the polymerization, 0.1% ammonium persulfate (APS) and 0.1% of tetramethylethylenediamine (TEMED) were mixed in the gel solutions and 20 μL of the mixture was pipetted onto hydrophobically treated glass slides. After polymerization, the gels on the coverslips were detached and treated with hydrazine hydrate 55% for 2 h with rocking [36]. 5% Glacial acetic acid for 1 h and then distilled water for 1 h were used to rinse hydrazine and glacial acetic acid, respectively. Polydimethylsiloxane (PDMS, Polysciences, Inc.) stamps were produced by conventional polymerization methods. Sodium periodate (~3.5 mg/mL) was used to generate free aldehydes on matrix proteins and added to 25 μg/mL of fibronectin in PBS for at least 45 min. The protein solution was pipetted onto patterned stamps for 30 min and dried with air. Free aldehydes in proteins were chemically conjugated with reactive hydrazide groups on the gels, resulting in transferring the protein residue on the stamps to the gel surfaces [36].

2.3. Cell source and culture

Human MSCs were purchased from Lonza. The MSCs were harvested and cultured from normal bone marrow. Cells were positive for CD105, CD166, CD29, and CD44 and negative for CD14, CD34 and CD45 by flow cytometry (http://www.lonza.com). Purchased MSCs from bone marrow were cultured and then expanded cells were frozen in cryopreservation (10% DMSO) with passage 2. Cells were thawed and cultured in Dulbecco's Modified Eagle's Medium (DMEM) low glucose (1 g/mL) media supplemented with 10% fetal bovine serum (MSC approved FBS; Invitrogen), and 1% penicillin/streptomycin (p/s). Media was changed every 3 or 4 days. Passage 4–8 MSCs were seeded on patterned surfaces at a cell density of ~5000 cells/cm^2. MSCs were cultured for 10 days before analysis.

2.4. Immunocytochemistry and histology

Cells on surfaces were fixed with 4% paraformaldehyde (Alfa Aesar) for 20 min. To permeabilize cells, 0.1% Triton X-100 in PBS was employed for 30 min. Cells were blocked with 1% bovine serum albumin (BSA) for 15 min and labeled with primary antibody in 1% BSA in PBS for 2 h at room temperature (20 °C) with mouse anti-MyoD, α5β1, or αVβ3 and rabbit anti-Runx2 or Osteopontin (1:500 dilution). Secondary antibody labeling was performed by the same procedure with Tetramethylrhodamine-conjugated anti-rabbit IgG antibody, Alexa Fluor 488-phalloidin (1:200 dilution), Alexa647-conjugated anti-mouse IgG antibody, and 4,6-diamidino-2-phenylindole (DAPI, 1:5000 dilution) for 20 min in a humid chamber (37 °C). Immunofluorescence microscopy was conducted using a Zeiss Axiovert 200 M inverted research-grade microscope (Carl Zeiss, Inc.). Immunofluorescent images were analyzed using ImageJ; the fluorescence intensity of single cells (over 20 cells) for each condition was measured to compare different levels of marker expression. To stain for alkaline phosphatase, surfaces were rinsed with distilled water and incubated for 30 min in BCIP/NBT solution, rinsed well in PBS and imaged in bright field using a Motic trinocular inverted microscope. All experiments were repeated at least three times. Only single cells that were captured in patterns were used in the analysis. The relative intensity of the fluorescence was determined by comparing each intensity value to the average intensity of one condition. For Figs. 2, 3 and 6, average marker intensities of circular cells in 5000 μm^2 patterned stiff (10 kPa) substrates were selected. For Fig. 5, average mRNA expressions of cells in 5000 μm^2 circle patterned (10 kPa) substrates were selected. The intensity value for single cells was obtained from nuclei (Runx2 and MyoD) or cytoplasmic (Osteopontin) staining intensity minus backgrounds.

2.5. Traction stress measurement

Polyacrylamide gels with desired stiffness (10 and 30 kPa) were fabricated on a glass cover slip (18 mm) as described above [29]. To obtain fluorescent bead-infused gels, the polyacrylamide solution was mixed with a 1 μm-bead suspension (Invitrogen, F-8821) at 1:250 and a small amount (1~2 μl) was applied to gel solutions. Upon the placement of the gel surface faced down, beads in a single layer at the same focal plane were imaged using a fluorescent microscope. Matrix proteins were patterned as described above. An Olympus IX81 fluorescent microscope and 20× objective was used to obtain the live cell images [37]. Throughout the experiment, temperature and carbon dioxide levels were maintained at 37 °C and 5% respectively. Live cell images on gels embedded with fluorescent beads were captured. Bright field images were firstly taken of the cells to visualize cell shape and location, and then fluorescent images of beads were taken. In order to assess the displacement of beads under the null-force condition, cells were removed from the surface using sodium dodecyl sulfate (SDS, Fisher Inc.), resulting in the gel returning to its relaxed initial state without cells. To

characterize the gel displacements, the images before and after cell removal were analyzed using Matlab digital image correlation programs published in Ref. [37] to obtain the 2D displacement field (ux, uy). The resolution of the algorithm is 1/10 of pixel size, i.e. ~33 nm, and signal-to-noise ratio reaches 40. The detailed procedures of cell traction computation using finite element method can be found in a previous report [37]. In brief, our computation employed a mixed boundary condition model, by prescribing zero traction at all nodes outside the cell (Fx = Fy = Fz = 0) and the obtained 2D displacement field (ux, uy) as well as Fz = 0 at the nodes within the cell boundaries. We did not measure uz during the experiments. Our theoretical derivation suggests that for elastic biomaterial substrates with Poisson's ratio close to 0.5, such as PA gels, prescribing Fz = 0 for all surface nodes results in an error of less than 2% in the calculation of in-plane forces Fx and Fy [37].

2.6. RNA isolation and RT-PCR

Adherent cells were lysed directly in TRIZOL reagent (Invitrogen). Chloroform extraction and ethanol precipitation were employed to isolate total RNA. Total RNA was reverse transcribed using Superscript III® First Strand Synthesis System for RT-PCR (Invitrogen). RT-PCR was achieved linearly by cycle number for each primer set using SYBR® Green Real-Time PCR Master Mix (Invitrogen) on an Eppendorf Realplex 4S Real-time PCR system. Primer sequences were as follows: α1 CTC CTCACTGTTGTTCTACGCT and ATCCAAACATGTCTTCCACCG, α3 CCCACCTGGTGTGACTTCTT and TCCCTGGAGGTGGGTAGC, α5 TGCCGAGTTCACCAAGACTG and TGCAATCTGCTCCTGAGTGG, αv CATCTTAATGTTGTGCCGGATGT and TCCTTCCACAATCCCAGGCT, α6 CAACTTGGACACTCGGGAGG and ACGAGCAACAGCCGCTT, β1 CCGCGCGGAAAAGATGAATTT and AGCAAACACACAGCAAACTGA, β3 TTGGAGACACGGTGAGCTTC and GCCCACGGGCTTTATGGTAA, GAPDHTGCCTCGATGGGTGGAGT and GCCCAATACGACCAAATCAGA. All reactions were performed linearly by cycle number for each set of primers.

2.7. Inhibition assays

Inhibitors were added to cell culture media at the following concentrations before and after cell seeding and with each media change: Blebbistatin (1 μM) and Y-27632 (2 μM) (Calbiochem). Integrin blocking antibodies (α5β1 and αvβ3) were added to cells in media prior to deposition at 1 μg/mL. MAP kinase inhibition was performed by adding supplemented media of the following molecules at 6 μM after cell seeding and with each media change: FR180204 (ERK1/2), SP600125 (JNK), and SB202190 (p38).

2.8. Statistical analysis

Error bars represent standard deviation and N value is the number of experimental replicates. For statistical analysis one-way ANOVA for comparing multiple groups and two-tailed p-values from unpaired t-test for comparing two groups were employed and values of $P < 0.05$ were considered statistically significant.

3. Results

3.1. Single cell patterning with adhesive proteins on polyacrylamide hydrogels of different stiffness

We used microcontact printing of adhesive proteins (fibronectin, laminin and collagen) on polyacrylamide (PAAm) hydrogels as a flexible platform to investigate the combinatorial effects of substrate elasticity, matrix composition and cell shape in controlling osteogenesis and myogenesis on protein-coated hydrogels (Fig. 1a). Polydimethylsiloxane (PDMS) stamps were fabricated

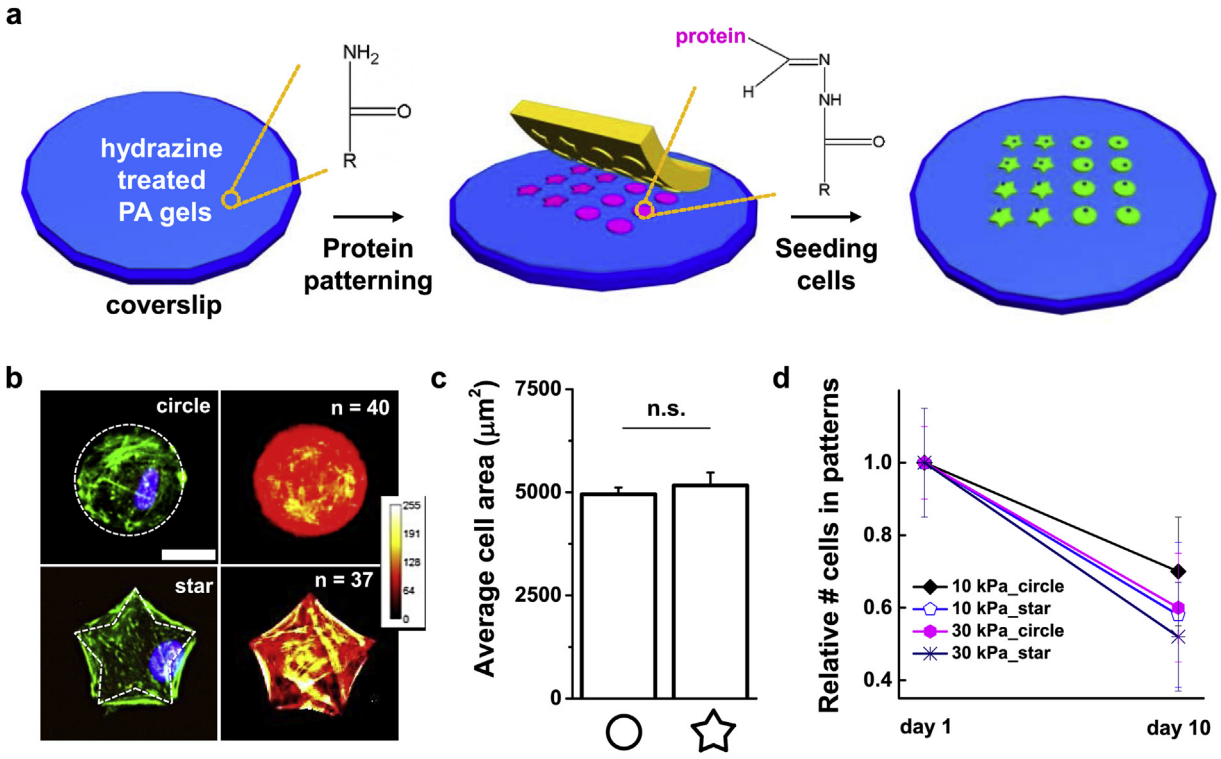

Fig. 1. Single cell patterning on hydrogels can be achieved by protein immobilization with hydrazine hydrate chemistry. (a) Schematic of the procedure for patterning cells on polyacrylamide hydrogels. (b) Representative immunofluorescence microscopy images and heat maps of MSCs on circle and star shapes. Staining for MSC nuclei (blue), actin (cyan-green). Scale bar is 40 μm. (c) MSC area on patterned protein-coated hydrogels after 10days. (d) Relative number of cells in patterns after 10 days. (For interpretation of the references to colour in this figure legend, the reader is referred to the web version of this article.)

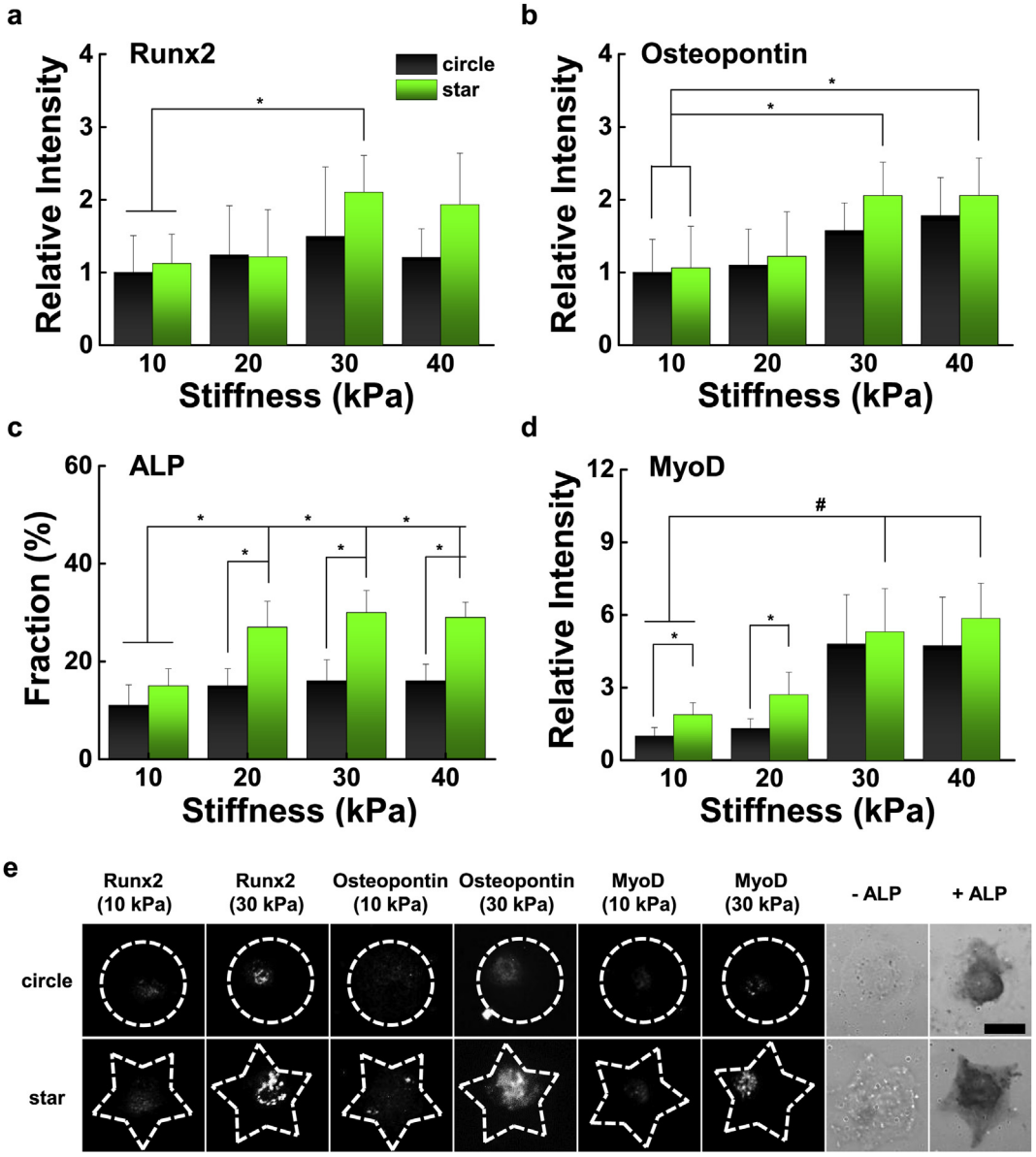

Fig. 2. Combinations of matrix stiffness and geometric features guide osteogenesis and myogenesis. Expression of osteogenic (a)–(c) and myogenic (d) markers for cells adherent to the circle or star shape patterned fibronectin coated substrates demonstrating how combinations of matrix stiffness and geometric features influence differentiation. (e) Immunofluorescence image of MSCs stained with Runx2, Osteopontin, ALP, or MyoD. Scale bar is 40 μm. Error bars are standard deviations (N = 4). (*P < 0.05 and #P < 0.01, one-way ANOVA).

using photolithography and used to pattern adhesive islands of proteins on the surface of chemically modified hydrogels. We employed two different shapes of identical area for patterning the hydrogels, one a simple circle and one approximating a star, where the cell body is expected to span non-adhesive regions [19]. PAAm hydrogels with a range of stiffness (10–40 kPa) were prepared as previously reported [29]. This range of stiffness is physiologically relevant with 10 and 30 kPa stiffness mimicking the rigidity of muscle or pre-calcified bone tissue, respectively [17]. The surfaces of PAAm gels were chemically modified with hydrazine hydrate [36], which allows for covalent immobilization between the treated gel surface and an oxidized glycoprotein solution via microcontact printing. After seeding, the mesenchymal stem cells (MSCs) attached and conformed to the patterned regions. To explore the influence of cell shape on the distribution of the cytoskeleton, we fixed and stained the patterned cultures for filamentous actin. Fig. 1b shows actin stains and heatmaps of >30 cells per shape which demonstrates classical cortical actin patterns for MSCs in circles, while MSCs in a star shape show pentagonally organized regions of actin stress fibers. Morphological analysis reveals that the patterned cells that adhere to the printed area show a comparable size to the defined patterns (5000 μm^2) (Fig. 1c). Patterned cells stayed viable and maintained adhesion to the islands for 10 days in culture, but a higher number of cells on stiffer substrates and patterns with higher actomyosin contractility escaped from geometric confinement and proliferated (Fig. 1d).

3.2. *The influence of cell shape, matrix stiffness and composition during mesenchymal stem cell differentiation*

First we investigated osteogenic and myogenic marker expressions of MSCs cultured in the different shapes on fibronectin-

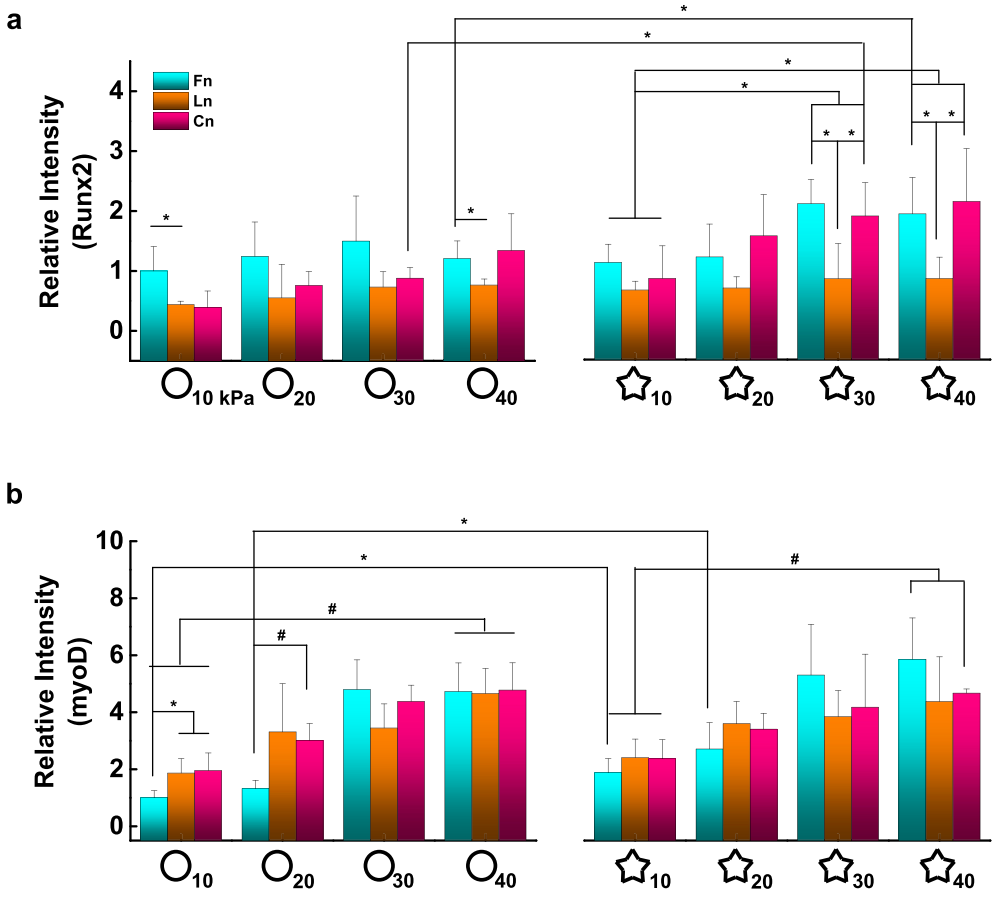

Fig. 3. Cell shape, matrix elasticity, and composition all influence differentiation. Quantitation of (a) Runx2 and (b) MyoD markers for patterned cells cultured on different adhesive proteins coated substrates with tunable stiffness for 10 days. Error bars are standard deviations (N = 4). (*P < 0.05 and #P < 0.01, one-way ANOVA).

coated hydrogels of varying stiffness (~10–40 kPa). We used three different osteogenic markers (Runx2 and ALP as early osteogenic markers; Osteopontin as a late osteogenic marker) and a myogenic marker (MyoD) to compare the degree of osteogenesis and myogenesis specification depending on matrix stiffness and cell shape after 10 days in culture (Fig. 2). Cells cultured on substrates with different stiffness express markers associated with osteogenesis and myogenesis in a stiffness dependent manner with a maximum at ~30–40 kPa. In addition, cells in star shapes show higher levels of osteogenic and myogenic marker expressions compared to those cultured in circular shapes. We also explored alternative shapes previously shown to influence actomyosin contractility: oval shapes with different aspect ratios (1:1, 2:1, 4:1, 8:1, and 12:1, 5000 μm^2) (Fig. S1). Similar to cells on circle and star shapes, those on shapes that promote higher contractility express higher levels of osteogenic markers. Next we patterned our two shapes using different matrix proteins (fibronectin, laminin and collagen) across surfaces with different stiffness to explore how these cues influence lineage specification when presented in combination (Fig. 3). We used representative osteogenic (Runx2) and myogenic (MyoD) transcription factors to assess early differentiation to these lineages. Cells cultured on fibronectin or collagen matrices show increased Runx2 expression as substrate stiffness is increased, while MSCs cultured on laminin did not show a trend in differentiation on account of substrate stiffness. In contrast, MSC myogenesis was shown to be sensitive to substrate stiffness across all matrices. Changing the geometry of single MSCs from a circular shape to that approximating a star led to increased expression of Runx2 (fibronectin and collagen) and MyoD (fibronectin). However, similar to stiffness the shape of single cells on laminin did not influence osteogenesis.

3.3. The role of biophysical and biochemical parameters in guiding mesenchymal stem cell traction stress

Micropatterning single cells allows precise control over adhesive structures, and we postulated that the way in which MSCs deform their matrices would be influenced by shape, stiffness and protein composition. First, to explore the relationship between substrate mechanics, adhesion and differentiation, we measured the traction stress exerted by circular and star-shaped MSCs on hydrogels of two different stiffness (10 and 30 kPa), across three different matrix proteins (fibronectin, laminin, and collagen) (Fig. 4). We observed that cells on star shapes on a fibronectin matrix showed higher traction stresses than those on laminin (2.5-fold on 10 kPa; 7.2-fold on 30 kPa) or on collagen (4.3-fold on 10 kPa; 10.3-fold on 30 kPa). For the same shape and adhesive proteins, matrix stiffness gave rise to different levels of traction stresses; star shaped cells on fibronectin coated 30 kPa substrates displayed 3.2-fold higher traction stresses than those on 10 kPa gels. In addition, MSCs tended to exert higher traction when they were cultured in star geometries on a fibronectin matrix (6.4-fold or 7.5-fold higher than circular cells on 10 or 30 kPa, respectively). However, traction exerted by cells on laminin substrates displayed no significant difference (within the limitations of small sample size) even when cultured on different stiffness or in the contractile star geometry. While stiffness influenced the MSCs' ability to exert traction on collagen coated gels, there was no discernible influence of cell shape.

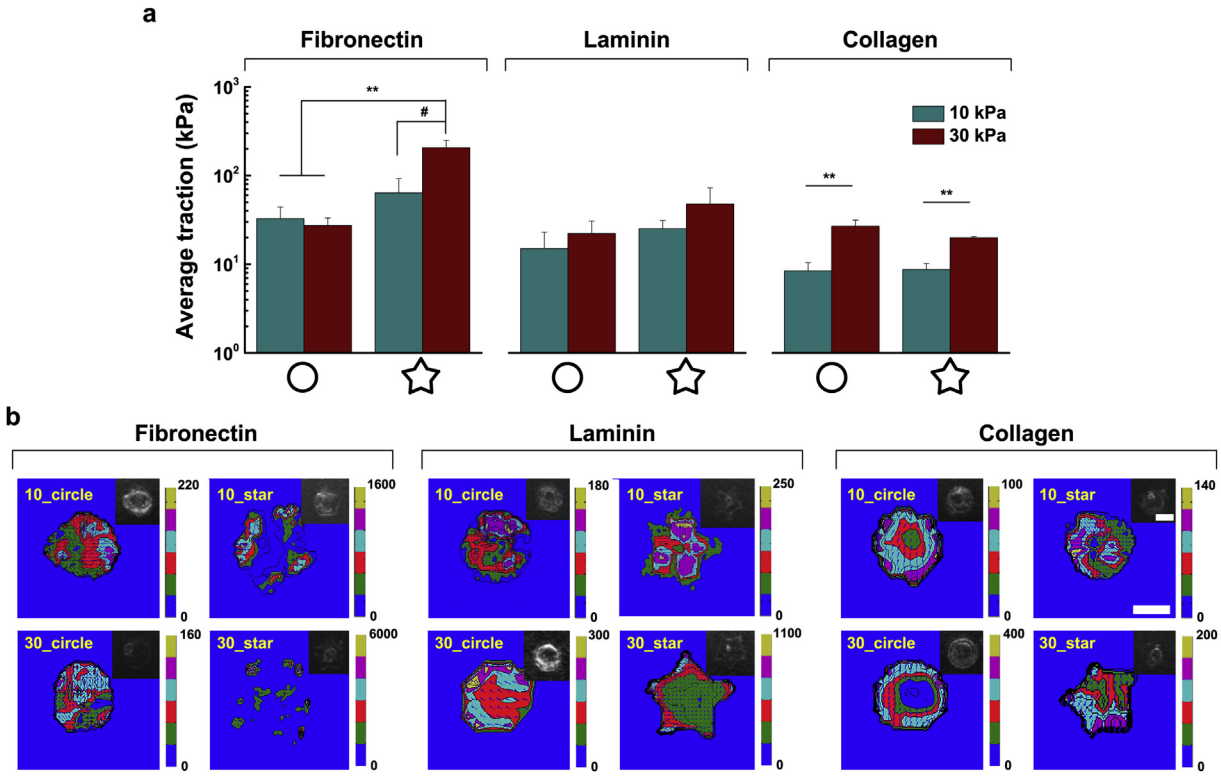

Fig. 4. Traction stress exerted by MSCs is influenced by combinations of biophysical and biochemical cues. (a) Average cellular traction stress for MSCs after 1 day of culture. (b) Representative traction map and phase-contrast image (inserted) of MSCs cultured for 1 day. The cells were cultured on combinations of matrix stiffness (10 and 30 kPa), cell shape (circle and star), and adhesive protein (fibronectin, laminin, and collagen). Scale bar is 40 μm. Error bars are standard deviations (N = 3). ($^{\#}P < 0.01$ and $^{**}P < 0.005$, one-way ANOVA).

3.4. The expression of integrin receptors in response to cell geometry and matrix stiffness

Since MSCs cultured on fibronectin show clear differences in both differentiation and traction stress as a function of matrix stiffness and cell shape, we analyzed the expression of common integrin receptors involved in fibronectin recognition. Cells were cultured for 1 day on matrices of different stiffness (10 or 30 kPa) and in different geometries (circle or star shape) followed by lysis, RNA isolation and RT-PCR. Interestingly, MSCs cultured in the star shape show higher expression than MSCs cultured in circular shapes on both 10 kPa hydrogels (2.3-fold α1, 3.1-fold α3, 2.1-fold α5, 73-fold αv, 3.3-fold α6, 2.1-fold β1, 5.5-fold β3; Fig. S2) and 30 kPa (1.2-fold α1, 2.7-fold α3, 2.7-fold α5, 261.3-fold αv, 2.5-fold α6, 2.1-fold β1, and 2.6-fold β3; Fig. 5). In general integrin expression is higher for cells cultured in the star shape, but in particular integrin αv shows an enormous increase in expression for culture in the star geometry compared to the circle in both 10 and 30 kPa

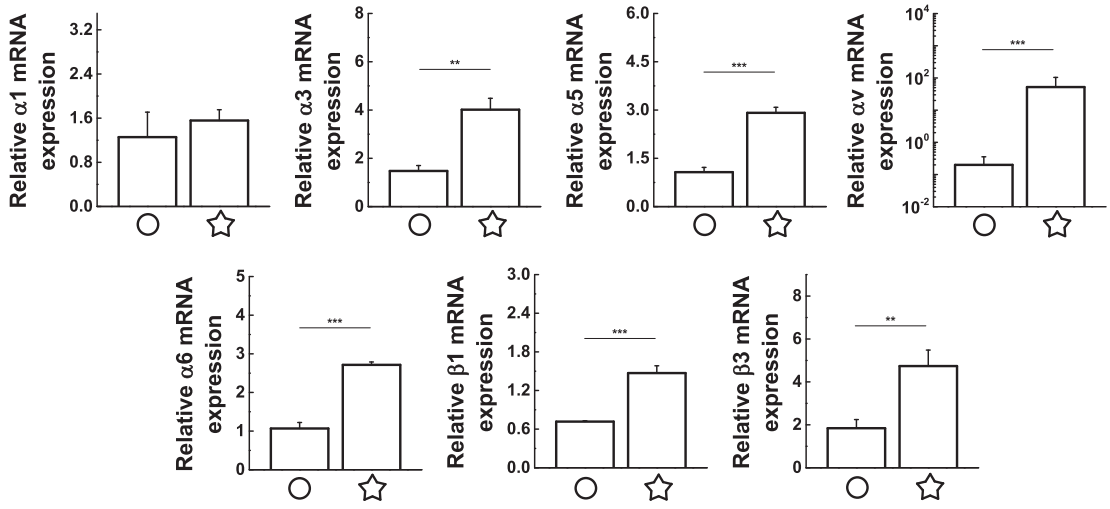

Fig. 5. Gene expression analysis of integrins for patterned mesenchymal stem cells on fibronectin coated 30 kPa substrates. Results of real-time PCR to measure the gene expression of integrin α1, α3, α5, αv, α6, β1, and β3 of MSCs cultured for 1 day Error bars are standard deviations (N = 3). ($^{**}P < 0.005$ and $^{***}P < 0.0005$, one-way ANOVA).

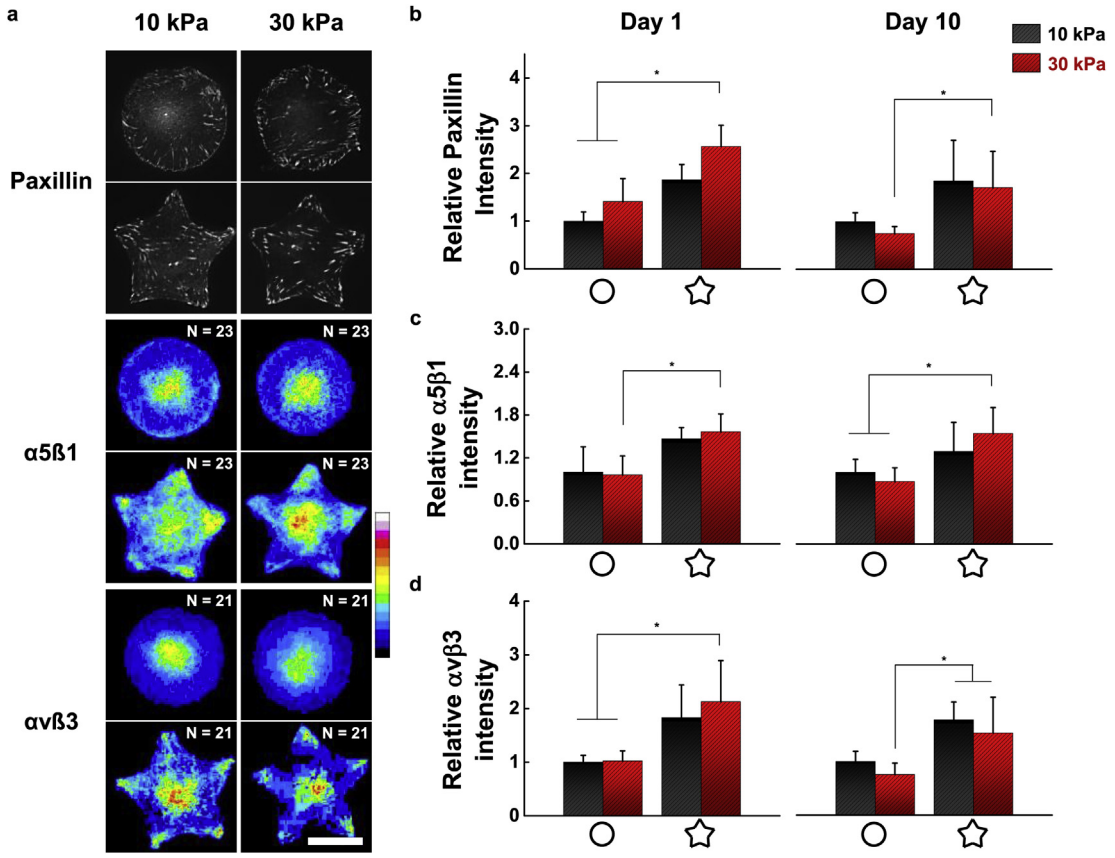

Fig. 6. Focal adhesion architecture and integrin composition is guided by cell shape and substrate stiffness. (a) Immunofluorescence image of MSCs cultured for 10 days stained with Paxillin and heat maps of MSCs for integrin α5β1 and αvβ3. Scale bar is 40 μm. (b) Quantitation of Paxillin and integrin α5β1 and αvβ3 markers for patterned cells cultured on fibronectin coated 10 and 30 kPa substrates for 1 and 10 days. Error bars are standard deviations (N = 3). (*P < 0.05, one-way ANOVA).

fibronectin conjugated hydrogels.

To further verify the observed trends in integrin expression, we performed immunofluorescence staining of a focal adhesion marker (Paxillin) and two major integrin receptors in fibronectin (α5β1 and αvβ3) (Fig. 6 and S3). Protein expression by immunofluorescence showed the same trend as the RT-PCR study: higher levels of focal adhesion and integrin expression for MSCs cultured in star shapes compared to those in circular shapes. Since we cultured MSCs for 10 days to study lineage specification and differentiation, we also measured paxillin, α5β1, and αvβ3 at day 10. Similar to cells cultured for 1 day, MSCs cultured for 10 days on star shaped fibronectin substrates displayed higher levels of focal adhesion proteins and integrin receptors.

3.5. Blocking integrin receptors and downstream signaling during differentiation of mesenchymal stem cells

MSCs cultured in star shapes show enhanced traction stress, integrin expression, and lineage specification to both osteogenesis and myogenesis programs. To elucidate signal transduction pathways that are involved in linking extracellular recognition to differentiation, we treated our patterned cultures with mitogen activated protein kinase (MAPK) inhibitors (p38, ERK1/2, and JNK), the Rho-associated kinase inhibitor Y-27632, the non-muscle myosin inhibitor blebbistatin, and integrin blocking antibodies for α5β1 and αvβ3. MSCs were cultured in 5000 μm^2 star geometries with or without 6 μM p38, ERK1/2, and JNK, 2 mM Y-27632, 1 mM blebbistatin, or 1 μg/mL anti-α5β1 and anti-αvβ3 for 10 days. We employed early (Runx2) and late (Osteopontin) osteogenic markers to investigate the effects of inhibitors on different stages of differentiation (Fig. 7). The expression of Runx2 shows a modest decrease after treatment with pharmacological inhibitors and blocking antibodies; however, the later marker Ostopontin shows a decreases on account of both blocking integrins and inhibiting downstream signal transduction players. Blocking integrin α5β1 in particular shows decreased expression of both Runx2 and Osteopontin, which suggests that signaling through this integrin plays a significant role during osteogenesis on these matrices.

4. Discussion

Cell surface integrin receptors sense the biophysical and biochemical properties of the extracellular matrix, convey this information to the interior of the cell, and regulate gene expression during stem cell differentiation [10,13]. While the bulk mechanics of the extracellular matrix (ECM) clearly plays a role during lineage specification of stem cells on deformable substrates [17,20,30], the identity of the tethered protein will influence the way in which integrin receptors can exert force on the matrix, establish focal adhesions, and transduce this mechanical and biochemical information to the nucleus [38]. Discerning the relationship between integrin mediated traction, focal adhesion, and the mechanochemical signals that direct stem cell differentiation will prove useful for informing the design of the biomaterials interface.

To parse out the relative roles of biophysical and biochemical cues during MSC differentiation, we employed polyacrylamide hydrogels of four stiffness (10–40 kPa), three different conjugated matrix proteins (fibronectin, laminin, and collagen I), and two

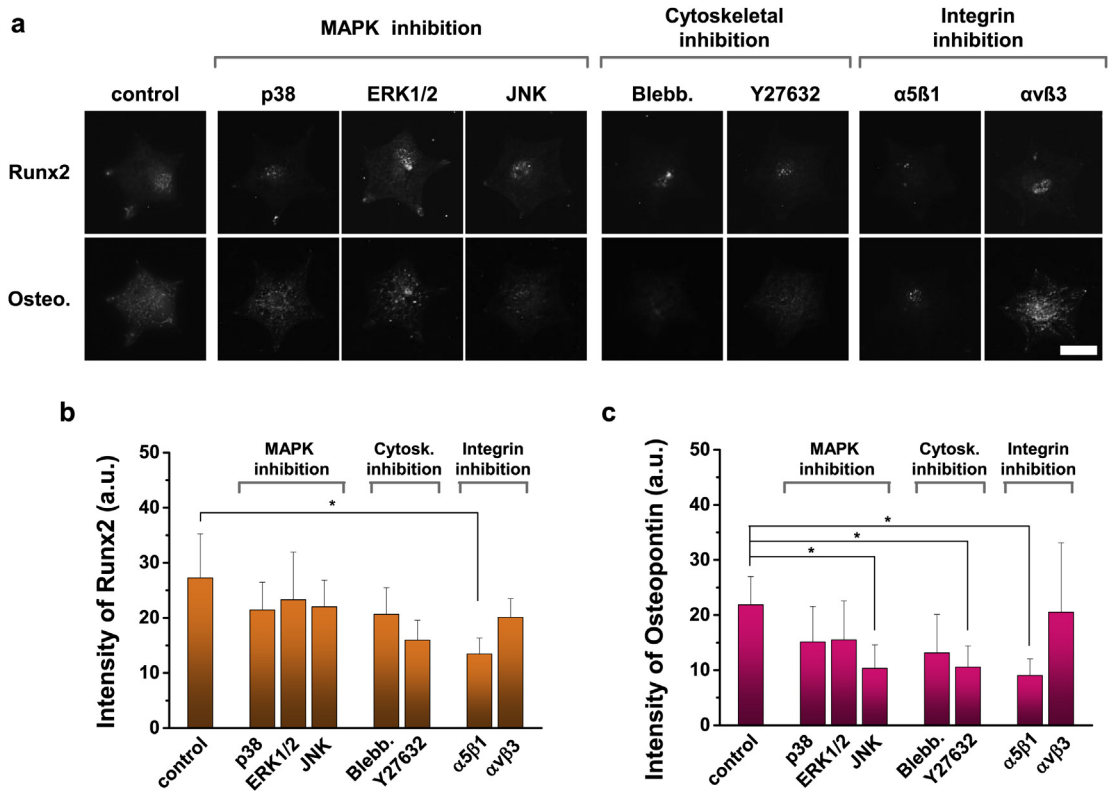

Fig. 7. Inhibition of integrins and downstream effectors influence differentiation. (a) Immunofluorescence image of MSCs stained with Runx2 and Osteopontin with or without inhibitors on 30 kPa substrates. Expression of early (Runx2) and late (Osteopontin) osteogenic markers for cells adherent to the star shape of fibronectin patterned substrates displaying how integrin α5β1 plays a critical role in osteogenic differentiation of MSCs. Scale bar is 40 μm. Error bars are standard deviations (N = 3). (*P < 0.05, one-way ANOVA).

distinct single cell shapes of the same area, but with different geometric cues for guiding subcellular structures (circle and star). In general, cells on stiffer substrates tend to express higher levels of osteogenesis markers. However, when other microenvironment cues are considered, e.g. tethered matrix proteins or control of single cell shapes, our data suggest that the trend in lineage specification can be tuned. For instance, cells on laminin coated surfaces show very little change in osteogenic marker expression regardless of stiffness and geometry. Round cells show similar expression levels of osteogenic markers while cells on star shapes—which coordinate focal adhesion and formation of stress fibers—tend to express higher levels in a stiffness dependent manner. These results show osteogenic differentiation can be modulated with specific combinations of these cues. In contrast, the degree of myogenesis gene expression depends less on single cell geometry and more on stiffness and matrix proteins.

Cells in vivo exert a 3D tensional homeostasis which controls diverse biological activities including stem cell differentiation [31,39]. Focal adhesions function as one of the intermediators of tension between cells and the ECM [17,19]. As cells exert traction stresses on deformable matrices, focal adhesions are reinforced and there have been several reports that size, density and turnover of focal adhesions influence differentiation [40,41]. As cells were cultured on our patterned matrices that differentially affect lineage outcome, we employed traction force microscopy (TFM) to determine the tractions exerted by MSCs by obtaining measurements of the micro-bead displacement within PAAm hydrogels [37]. MSCs cultured on fibronectin matrices were able to exert higher traction stress than cells adherent to laminin or collagen. This is consistent with previous reports that demonstrate a higher prevalence of fibronectin-binding integrins expressed in MSCs compared to those associated with laminin or collagen [42]. Furthermore, increasing cell perimeter by changing the geometry from a circle to a star leads to enhanced traction on fibronectin. In contrast, the traction exerted by MSCs on laminin and collagen matrices was not altered significantly as stiffness or cell geometry was changed. Coupled with the differentiation results, this study suggests that the ability of MSCs to exert traction through robust focal adhesions on fibronectin can guide the osteogenesis and myogenesis programs.

MSCs express multiple types of integrins involved in adhesion to fibronectin, and we found that cells cultured in star shapes showed higher expression of all integrins analyzed including α1, α3, α5, αv, α6, β1, and β3, irrespective of matrix stiffness. Remarkably, expression of integrin αv was 73-fold and 261-fold higher for cells cultured in star shapes on 10 kPa and 30 kPa hydrogels respectively. The enhancement in αv expression with changes in cell shape may be related to geometric guidance of adhesion structures and force transmission to modulate outcome through mechanotransduction [43–45]. Immunostaining MSCs in circle and star shapes for integrin α5β1 and αvβ3 demonstrates an increase in expression at the protein level for both integrins. Therefore we propose that both α5β1 and αvβ3 are likely involved in in vitro focal adhesion formation, traction generation and regulation of differentiation for MSCs cultured on deformable matrices.

To evaluate the role of these integrins in mediating differentiation, we added blocking antibodies to the cell culture media. While inhibition of αvβ3 leads to a slight decrease in early osteogenesis marker expression (Runx2), inhibition of α5β1 shows a large decrease in both early (Runx2) and late (osteopontin) marker expression. Integrins are known to be involved in stem cell lineage specification. For example, integrin α5 promotes osteogenic differentiation of MSCs [10,46]. Integrin α5 was up-regulated during

osteogenesis and down-regulated with shRNAs inhibiting osteogenic differentiation, and the osteogenic differentiation enhanced by integrin α5 was related to the focal adhesion kinase/ERK1/2-MAPKs and PI3K signaling pathways [46]. Roca-Cusachs et al. reported that two main fibronectin receptors, α5β1 and αvβ3, play a different role in cell adhesion [47]. Adhesion strength was dependent on the clustering of integrin α5β1 while αvβ3, which is less stable, mediates mechanotransduction and integrin-cytoskeleton interactions. This result is in line with our data for MSCs with different shapes on fibronectin; cells on star shapes showed higher levels of these integrins and accordingly higher traction stresses and osteogenic outcomes than those on circular shapes. We speculate that both integrins are involved in adhesion, but with disparate roles: αvβ3 in mediating focal adhesion assembly through bi-directional force transmission, and α5β1 in regulating the differentiation program through mechanotransduction. Adding pharmacological inhibitors of downstream effectors of integrin signaling, including Rho-associated protein kinase, non-muscle myosins, and extracellular related MAP kinases p38, ERK 1 and 2, and c-Jun N-termina kinases, all show some decrease in osteogenesis markers. However, not to the same degree as to when initial adhesion via α5β1 is perturbed.

5. Conclusion

Using micropatterning we can precisely control the shape of single cells, thereby allowing the subcellular adhesive and contractile elements to be modulated. Using this strategy we show how matrix mechanics and adhesive protein composition can influence the way in which MSCs exert traction stresses during differentiation in response to deformable matrices. In particular, MSCs cultured on fibronectin modified hydrogels of increasing stiffness display higher levels of traction, increased expression of integrin receptors, and an increased propensity to differentiate, when they are in geometries that promote enhanced focal adhesion and a contractile cytoskeleton. Using integrin blocking antibodies and pharmacological inhibitors of downstream effectors, we demonstrate that MSCs adhere and deform the fibronectin conjugated matrices through both αvβ3 and α5β1 integrins; however, osteogenesis is directed primarily through integrin α5β1. By careful control of multiple biochemical and biophysical parameters, the relationship between integrin mediated adhesion, deformation of the extracellular matrix, and regulation of distinct differentiation programs can be discerned, and may find broad applicability across a range of cell systems.

Disclosures

The authors indicate no potential conflicts of interest.

Acknowledgments

This work was supported by the National Heart Lung and Blood Institute of the National Institutes of Health, grant number HL121757.

Appendix A. Supplementary data

Supplementary data related to this article can be found at http://dx.doi.org/10.1016/j.biomaterials.2015.08.005.

References

[1] L. Li, T. Xie, Stem cell niche: structure and function, Annu. Rev. Cell Dev. Biol. 21 (2005) 605–631.
[2] D.L. Jones, A.J. Wagers, No place like home: anatomy and function of the stem cell niche, Nat. Rev. Mol. Cell Biol. 9 (2008) 11–21.
[3] Y.-K. Wang, C.S. Chen, Cell adhesion and mechanical stimulation in the regulation of mesenchymal stem cell differentiation, J. Cell Mol. Med. 17 (2013) 823–832.
[4] F. Guilak, D.M. Cohen, B.T. Estes, J.M. Gimble, W. Liedtke, C.S. Chen, Control of stem cell fate by physical interactions with the extracellular matrix, Cell Stem Cell 5 (2009) 17–26.
[5] X. Yao, R. Peng, J. Ding, Cell-material interactions revealed via material techniques of surface patterning, Adv. Mater 25 (2013) 5257–5286.
[6] S. Mitragotri, J. Lahann, Physical approaches to biomaterial design, Nat. Mater. 8 (2009) 15–23.
[7] J. Lee, A.A. Abdeen, A.S. Kim, K.A. Kilian, Influence of biophysical parameters on maintaining the mesenchymal stem cell phenotype, ACS Biomater. Sci. Eng. 1 (2015) 218–226.
[8] C. Huang, J. Dai, X.A. Zhang, Environmental physical cues determine the lineage specification of mesenchymal stem cells, Biochim. Biophys. Acta 1850 (2015) 1261–1266.
[9] S. Na, O. Collin, F. Chowdhury, B. Tay, M. Ouyang, Y. Wang, et al., Rapid signal transduction in living cells is a unique feature of mechanotransduction, Proc. Natl. Acad. Sci. U. S. A. 105 (2008) 6626–6631.
[10] J.E. Frith, R.J. Mills, J.E. Hudson, J.J. Cooper-White, Tailored integrin-extracellular matrix interactions to direct human mesenchymal stem cell differentiation, Stem Cells Dev. 21 (2012) 2442–2456.
[11] N.D. Gallant, K.E. Michael, J. Garcı, Cell Adhesion Strengthening: Contributions of Adhesive Area, Integrin Binding, and Focal Adhesion Assembly, vol. 16, 2005, pp. 4329–4340.
[12] C.S. Chen, M. Mrksich, S. Huang, G.M. Whitesides, D.E. Ingber, Geometric control of cell life and death, Science 276 (1997) 1425–1428.
[13] S. Gronthos, P. Simmons, S. Graves, P.G. Robey, Integrin-mediated interactions between human bone marrow stromal precursor cells and the extracellular matrix, Bone 28 (2001) 174–181.
[14] Y. Shao, J. Sang, J. Fu, On human pluripotent stem cell control: The rise of 3D bioengineering and mechanobiology, Biomaterials 52 (2015) 26–43.
[15] S. Khetan, M. Guvendiren, W.R. Legant, D.M. Cohen, C.S. Chen, J.A. Burdick, Degradation-mediated cellular traction directs stem cell fate in covalently crosslinked three-dimensional hydrogels, Nat. Mater 12 (2013) 1–8.
[16] L. Gao, R. McBeath, C.S. Chen, Stem cell shape regulates a chondrogenic versus myogenic fate through Rac1 and N-cadherin, Stem Cells 28 (2010) 564–572.
[17] A.J. Engler, S. Sen, H.L. Sweeney, D.E. Discher, Matrix elasticity directs stem cell lineage specification, Cell 126 (2006) 677–689.
[18] K. Kolind, K.W. Leong, F. Besenbacher, M. Foss, Guidance of stem cell fate on 2D patterned surfaces, Biomaterials 33 (2012) 6626–6633.
[19] K.A. Kilian, B. Bugarija, B.T. Lahn, M. Mrksich, Geometric cues for directing the differentiation of mesenchymal stem cells, Proc. Natl. Acad. Sci. U. S. A. 107 (2010) 4872–4877.
[20] J. Lee, A.A. Abdeen, D. Zhang, K.A. Kilian, Directing stem cell fate on hydrogel substrates by controlling cell geometry, matrix mechanics and adhesion ligand composition, Biomaterials 34 (2013) 8140–8148.
[21] A.S. Rowlands, P.A. George, J.J. Cooper-white, Directing Osteogenic and Myogenic Differentiation of MSCs: Interplay of Stiffness and Adhesive Ligand Presentation, 2008, pp. 1037–1044.
[22] P.C.D.P. Dingal, R.G. Wells, D.E. Discher, Simple insoluble cues specify stem cell differentiation, Proc. Natl. Acad. Sci. U. S. A. 111 (2014) 18104–18105.
[23] J.A. Burdick, W.L. Murphy, Moving from static to dynamic complexity in hydrogel design, Nat. Commun. 3 (2012) 1269.
[24] A.A. Abdeen, J.B. Weiss, J. Lee, K.A. Kilian, Matrix composition and mechanics direct proangiogenic signaling from mesenchymal stem cells, Tissue Eng. Part A 20 (2014) 2737–2745.
[25] W.L. Murphy, T.C. Mcdevitt, A.J. Engler, Materials as stem cell regulators, Nat. Mater 13 (2014) 547–557.
[26] J.S. Park, J.S. Chu, A.D. Tsou, R. Diop, Z. Tang, A. Wang, et al., The effect of matrix stiffness on the differentiation of mesenchymal stem cells in response to TGF-β, Biomaterials 32 (2011) 3921–3930.
[27] J. Fu, Y.-K. Wang, M.T. Yang, R a Desai, X. Yu, Z. Liu, et al., Mechanical regulation of cell function with geometrically modulated elastomeric substrates, Nat. Methods 7 (2010) 733–736.
[28] J. Lee, A.A. Abdeen, K.A. Kilian, Rewiring mesenchymal stem cell lineage specification by switching the biophysical microenvironment, Sci. Rep. 4 (2014) 5188.
[29] J. Lee, A.A. Abdeen, T.H. Huang, K.A. Kilian, Controlling cell geometry on substrates of variable stiffness can tune the degree of osteogenesis in human mesenchymal stem cells, J. Mech. Behav. Biomed. Mater 38 (2014) 209–218.
[30] A.S. Rowlands, P.A. George, J.J. Cooper-White, Directing osteogenic and myogenic differentiation of MSCs: interplay of stiffness and adhesive ligand presentation, Am. J. Physiol. 295 (2008) C1037–C1044.
[31] R. McBeath, D.M. Pirone, C.M. Nelson, K. Bhadriraju, C.S. Chen, Cell shape, cytoskeletal tension, and RhoA regulate stem cell lineage commitment, Dev. Cell 6 (2004) 483–495.
[32] R.O. Hynes, Integrins: versatility, modulation, and signaling in cell adhesion, Cell 69 (1992) 11–25.
[33] J.D. Humphries, A. Byron, M.J. Humphries, Integrin ligands at a glance, J. Cell Sci. 119 (2006) 3901–3903.
[34] U.R. Goessler, P. Bugert, K. Bieback, J. Stern-Straeter, G. Bran, K. Hörmann, et al., Integrin expression in stem cells from bone marrow and adipose tissue

during chondrogenic differentiation, Int. J. Mol. Med. 21 (2008) 271–279.
[35] J.R. Tse, A.J. Engler, Preparation of hydrogel substrates with tunable mechanical properties, Curr. Protoc. Cell Biol. 47 (2010) 10.16.1–10.16.16.
[36] V. Damljanović, B.C. Lagerholm, K. Jacobson, Bulk and micropatterned conjugation of extracellular matrix proteins to characterized polyacrylamide substrates for cell mechanotransduction assays, Biotechniques 39 (2005) 847–851.
[37] X. Tang, A. Tofangchi, S.V. Anand, T.A. Saif, A novel cell traction force microscopy to study multi-cellular system, PLoS Comput. Biol. 10 (2014) e1003631.
[38] N. Huebsch, P.R. Arany, A.S. Mao, D. Shvartsman, O a Ali, S a Bencherif, et al., Harnessing traction-mediated manipulation of the cell/matrix interface to control stem-cell fate, Nat. Mater 9 (2010) 518–526.
[39] M.L. Manning, R a Foty, M.S. Steinberg, E.-M. Schoetz, Coaction of intercellular adhesion and cortical tension specifies tissue surface tension, Proc. Natl. Acad. Sci. U. S. A. 107 (2010) 12517–12522.
[40] K.A. Kilian, M. Mrksich, Directing stem cell fate by controlling the affinity and density of ligand-receptor interactions at the biomaterials interface, Angew. Chem. Int. Ed. 51 (2012) 4891–4895.
[41] J.E. Frith, R.J. Mills, J.J. Cooper-White, Lateral spacing of adhesion peptides influences human mesenchymal stem cell behaviour, J. Cell Sci. 125 (2012) 317–327.
[42] L.A. Hidalgo-Bastida, S.H. Cartmell, Mesenchymal stem cells, osteoblasts and extracellular matrix proteins: enhancing cell adhesion and differentiation for bone tissue engineering, Tissue Eng. Part B 16 (2010) 405–412.
[43] J.D. Humphrey, E.R. Dufresne, M.A. Schwartz, Mechanotransduction and extracellular matrix homeostasis, Nat. Rev. Mol. Cell Biol. 15 (2014) 802–812.
[44] P.W. Oakes, M.L. Gardel, Stressing the limits of focal adhesion mechanosensitivity, Curr. Opin. Cell Biol. 30 (2014) 68–73.
[45] D. Riveline, E. Zamir, N.Q. Balaban, U.S. Schwarz, T. Ishizaki, S. Narumiya, et al., Focal contacts as mechanosensors: externally applied local mechanical force induces growth of focal contacts by an mDia1-dependent and ROCK-independent mechanism, J. Cell Biol. 153 (2001) 1175–1185.
[46] Z. Hamidouche, O. Fromigué, J. Ringe, T. Häupl, P. Vaudin, J.-C. Pagès, et al., Priming integrin alpha5 promotes human mesenchymal stromal cell osteoblast differentiation and osteogenesis, Proc. Natl. Acad. Sci. U. S. A. 106 (2009) 18587–18591.
[47] P. Roca-Cusachs, N.C. Gauthier, A. Del Rio, M.P. Sheetz, Clustering of α5β1 integrins determines adhesion strength whereas αvβ3 and talin enable mechanotransduction, Proc. Natl. Acad. Sci. U. S. A. 106 (2009) 16245–16250.